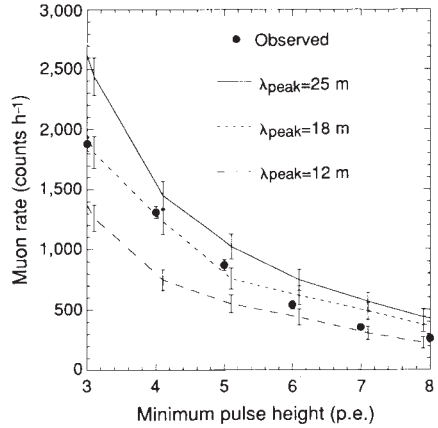


FIG. 3 Integral muon rate as a function of minimum pulse height (in p.e.) required of all three PMTs. Filled circles show experimental results, solid line shows Monte Carlo predictions if the Greenland ice has peak optical absorption length of 25 m (identical to laboratory ice). Dotted lines show Monte Carlo predictions for peak absorption lengths of 18 m and 12 m. The error bars show only statistical uncertainties in the observed rates and in the Monte Carlo rates.

observed presence of impurities in the butyl acetate used) would tend to reduce the predicted Monte Carlo rates, so our results should be regarded as a lower limit to the optical clarity of the ice. It should also be pointed out that the large absorption length implied by these results indicates that PMT size, rather than the optical quality of the ice, will be the limiting factor for a real neutrino detector: this is because for a smaller PMT, loss of light due to angular spread of the Cerenkov cone outweighs the loss of light due to optical absorption of the ice. Finally, because the ionic purity and particulate concentration of the Greenland ice are comparable to those measured for distilled water, it is not surprising that the optical properties of the two substances are also comparable. Trodahl and others[8] have studied the diffusive transport of light through bubbly sea ice and conclude that the optical absorption length at a wavelength of 500 nm must be at least 10 m; as this ice contains brine pockets and algae, the pure ice found in the interior of Greenland or Antarctica should be much better for our purposes.

We find these results very encouraging, and are planning more extensive experiments at the South Pole during the coming austral summer (November 1991–January 1992), in particular the operation of one or two strings, each with four 20-cm-diameter PMTs at a depth of ~1 km, where the ice is expected to be bubble free[9]. Assuming that these tests are successful, we then hope to begin construction and installation of full-size strings of twenty 20-cm-diameter PMTs in the succeeding season (1992–93). In addition, as part of this year's work, we will be investigating the possibility of using our detection technique to construct muon detectors able to operate in conjunction with South Pole Air Shower Experiment, an existing air-shower array at the South Pole[10]. The large effective muon-sensitive area of a PMT at shallower depths suggests that good muon coverage could be achieved with only a small number of drilled holes. □

Received 7 May; accepted 26 July 1991.

1. The DUMAND Collaboration *Rep. No.* HDC-3-88 (Hawaii DUMAND Center, 1988).
2. Barwick, S. W. *et al.* in *Proc. 3rd Int. Workshop on Neutrino Telescopes, Venice,* 1991 (in the press).
3. Halzen, F., Learned, J. & Stanev, T. *AIP Conf. Proc. 198* (eds Mullan, D. J. *et al*) 39–51 (American Institute of Physics, New York, 1988).
4. Miyake, S. *Proc. 13th International Cosmic Ray Conference* Vol. 5, 3638–3655 (University of Denver, Colorado, 1973).
5. Davis, G. E. *J. opt. Soc. Am.* **45,** 572–581 (1955).
6. Park, H. S. thesis, Univ. Michigan (1985).
7. Warren, S. G. *Appl. Optics.* **23,** 1206–1225 (1984).
8. Trodahl, H. J., Buckley, R. G. & Brown, S. *Appl. Optics* **26,** 3005–3017 (1987).
9. Gow, A. J. & Williamson, T. *Cold Regions Research and Engineering Laboratory Research Rep.* 339 (1975).
10. Smith, N. J. T. *et al. Nucl. Instrum. Meth. Phys. Res.* A**276,** 622–627 (1989).
11. Sullivan, J. D. *Nucl. Instrum. Meth.* **95,** 5–11 (1971).

ACKNOWLEDGEMENTS. We thank B. Koci and the entire PICO organization for the use of the borehole and for on-site assistance, E. K. Solarz and W. Williams for their help with the mechanical construction of the PMT string, J. Lynch and H. Zimmerman of the NSF, J. Learned for his sharing of DUMAND expertise, and E. Zeller of the University of Kansas for suggesting the idea of using South Pole ice in a neutrino telescope. This work was supported in part by the Division of Polar Programs of the US NSF and by the California Space Institute.

# The superconducting energy gap of $Rb_3C_{60}$

**Zhe Zhang, Chia-Chun Chen, Stephen P. Kelty, Hongjie Dai & Charles M. Lieber***

Department of Chemistry and Division of Applied Sciences, Harvard University, Cambridge, Massachusetts 02138, USA

**THE discovery of superconductivity in potassium-doped $C_{60}$ (ref. 1) has been followed by an intense effort to understand the physics and chemistry of metal-doped fullerene solids[2–13]. Experimental studies of alkali-metal-doped $C_{60}$ have now provided insight into the structure[7,13] and the coherence length and penetration depth[4] of the superconducting phase. No measurements of the superconducting energy gap ($\Delta$) have, however, been reported. The BCS theory of superconductivity[15], which has been used to interpret much of this experimental work[2,4,9–13], predicts (in the limit of weak coupling) that the reduced energy gap $2\Delta/kT_c$ has a material-independent value of 3.53. Values in excess of 3.5 define strong coupling, and thus provide insight into the nature of the pairing mechanism. Here we describe the measurement of $\Delta$ for single-phase superconducting $Rb_3C_{60}$ by tunnelling spectroscopy using a scanning tunnelling microscope. We obtain a value of $\Delta$ at 4.2 K of $6.6 \pm 0.4$ meV, corresponding to a reduced energy gap of 5.3. This is significantly larger than predicted by BCS theory, but similar in magnitude to values found for high-temperature copper oxide superconductors[14]. Our finding of strong coupling in $Rb_3C_{60}$ suggests the need for caution in using standard BCS theory to interpret superconductivity in metal-doped $C_{60}$.**

Tunnelling spectroscopy has been one of the most successful techniques used to probe conventional metal and alloy superconductors[16]. In particular, tunnelling spectra can provide values for both the energy gap $\Delta$ and the electron–phonon spectral function $\alpha^2F(\omega)$, where $\alpha^2$ is a measure of the coupling and $F(\omega)$ is the phonon density of states. To obtain a clear value for $\Delta$ by tunnelling, it is essential to prepare a uniform insulating barrier between the superconductor and metal junction. As the $C_{60}$ superconductors have short coherence lengths[4] and as the samples are inhomogenous, we expect that planar junctions might show significantly broadened gap features (even for the ideal BCS case). We have therefore used a low-temperature scanning tunnelling microscope (STM) to make point junctions with a sharpened metal tip. Point tunnelling spectroscopy has been used to measure $\Delta$ in a variety of superconducting materials, including pure metals[16], organics[17] and oxides[18], and the values of $\Delta$ determined by this technique for conventional superconductors are comparable to those obtained with planar junctions.

The $Rb_3C_{60}$ samples were prepared by methods described in detail elsewhere[12]. Briefly, purified and dried $C_{60}$ was reacted with RbHg in a 1:3 ratio at 200 °C for 8–72 h. After this initial reaction, the superconducting fraction determined from shielding measurements was typically >35%. The resulting powder was then ground, pressed into a pellet, and sintered at 200 °C for 3–12 h. Diamagnetic shielding measurements made on these sintered pellets show that the superconducting fraction can

* To whom correspondence should be addressed.

approach 100% of the sample volume. After characterization of a sintered pellet by magnetic susceptibility, it was mounted on the STM sample stage in an inert atmosphere glove box, and then transferred to the STM where it was contained in a vacuum chamber. Isolation of the sample is essential in these studies, as alkali-metal-doped $C_{60}$ decomposes on exposure to air and moisture[19]. The point junction was formed by mechanically moving a sharpened Pt-Ir alloy tip to the $Rb_3C_{60}$ pellet surface and then tuning the junction resistance with a piezoceramic positioner. Current against voltage ($I$-$V$) curves were recorded digitally using custom-built electronics under computer control. The sample temperature was actively controlled for $T > 4.2$ K.

The diamagnetic shielding curve for a typical $Rb_3C_{60}$ sintered pellet used in this study is shown in Fig. 1. The $T_c$ of this sample is 29 K and superconducting fraction is >60%; the large shielding fraction demonstrates that the sample is a bulk superconductor. After mounting a pellet in the STM, we recorded room-temperature $I$-$V$ curves to verify that the sample was metallic; that is, that it had not decomposed and become semiconducting[19]. The STM was then cooled to 4.2 K and tunnelling spectra were recorded at different locations on the sample. An $I$-$V$ curve recorded at 4.2 K on a high-quality sample is shown in Fig. 2*a*. This curve has a distinct zero-current regime about $V = 0$, and conductance sets in sharply at $\sim \pm 6$ mV. These features in the $I$-$V$ data are the characteristic signature of the superconducting energy gap. The gap structure was observed in most of the $I$-$V$ curves recorded at different locations on several high-quality samples. Occasionally we did not observe a gap; we believe, however, that such results are due to sample inhomogeneities (Z.Z. and C.M.L., unpublished data). An important observation is that the gap structure observed in Fig. 2*a* smears and then disappears as the sample temperature is increased above $T_c$ (Fig. 2*b*, *c*), and furthermore, that this structure then reappears when the sample is again cooled below $T_c$. As the gap structure is detected reproducibly below $T_c$ in high-quality superconducting samples, but disappears above $T_c$, it is clear that it can be assigned to the superconducting energy gap of $Rb_3C_{60}$.

We have quantitatively analysed the magnitude of $\Delta$ by calculating the conductance, $dI/dV$, as a function of voltage, since $dI/dV$ is proportional to the density of states. The conductance data determined from the $I$-$V$ curves show a gap in the density of states around $V = 0$ and conductance peaks at the gap edges (Fig. 3). These key features agree qualitatively with our expectations based on the low-temperature BCS expression for the energy gap, $dI/dV = eV/[(eV)^2 - \Delta^2]^{1/2}$, although the quantitative fit of this expression (solid curve, Fig. 3*a*) to our experimental data is not ideal. We note that the value of $\Delta$ determined from this fit, 6.8 meV, is significantly larger than that predicted by BCS theory, 4.41 meV. Deviations from the ideal BCS expression are often observed in tunnelling measurements[14] and could be due to inhomogeneity in our polycrystalline samples, or to broadening caused by inelastic scattering or strong coupling effects[16,17]. In addition, it is important to recognize that it is not known whether or not these new superconducting materials should show an ideal BCS energy gap, although BCS behaviour has been implicitly assumed in many analyses of experimental data[2,4,9-13]. To determine more accurately the value of $\Delta$ for $Rb_3C_{60}$, we account phenomenologically for deviations from the ideal BCS expression (Fig. 3*a*) by allowing for broadening as suggested by Dynes and coworkers: $dI/dV = \mathrm{Re}[|eV - i\Gamma|/((eV - i\Gamma)^2 - \Delta^2)^{1/2}]$, where $\Gamma$ is the broadening term[20]. Using this modified expression, we obtain good fits to our experimental $dI/dV$ data with $\Delta = 6.6$ meV and $\Gamma = 0.6$ meV (Fig. 3*b*). It is apparent from such fits that we have observed a 'BCS-like' energy gap in $Rb_3C_{60}$, and that the magnitude of $\Delta$ is substantially larger than predicted by weak-coupling BCS theory.

We therefore find from a number of independent experiments that $\Delta(4.2\ \mathrm{K}) = 6.6 \pm 0.4$ meV, that $\Delta$ becomes smaller as the temperature is increased (while remaining below $T_c$), and that

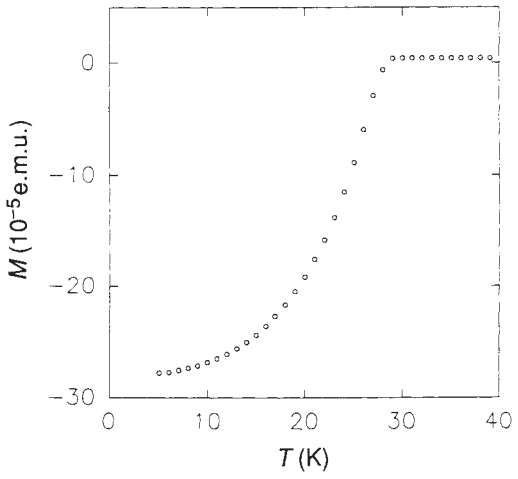


FIG. 1 Temperature dependence of the magnetization, $M$, obtained for a 3.1-mg $Rb_3C_{60}$ sintered pellet. The curve was recorded by cooling in zero field to 5 K and subsequent warming in a field of 5 Oe; $T_c = 29$ K. The sample was prepared by heating a pressed pellet of $Rb_3C_{60}$ powder for 3 h at 200 °C; the powder was first reacted at 200 °C for 72 h.

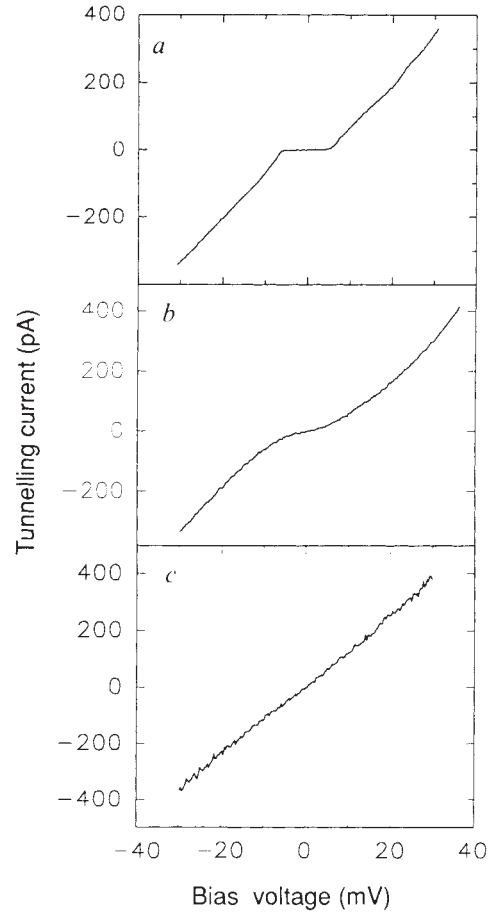


FIG. 2 Plots of $I$ (pA) against $V$ (mV) obtained on sintered pellet samples with a Pt-Ir alloy tip. The sample temperature in *a*, *b* and *c* was 4.2, 15 and 30 K, respectively. The samples for *b* and *c* were different from that in *a*.

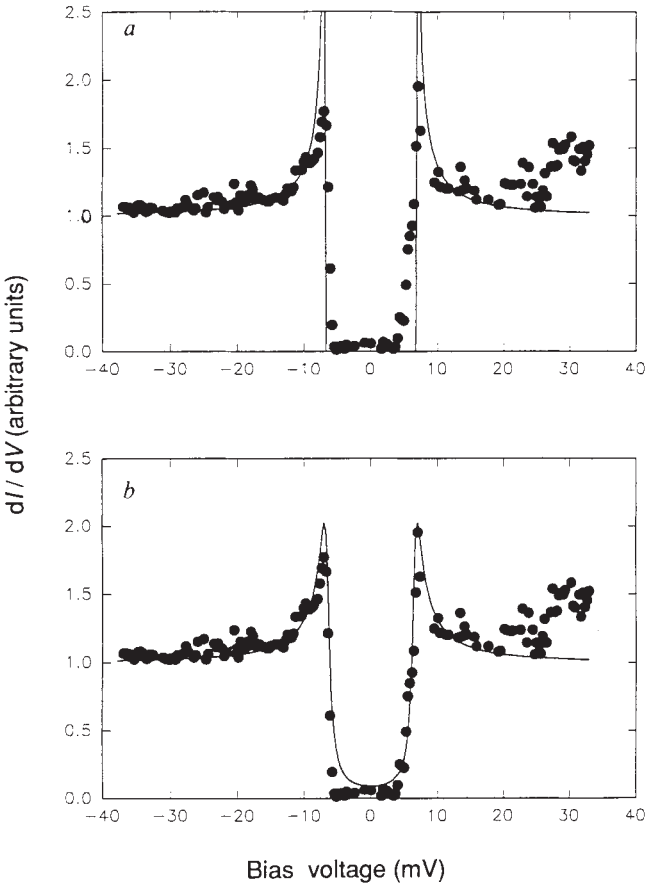


FIG. 3 Plots of d$I$/d$V$ against voltage (mV) for $Rb_3C_{60}$ at 4.2 K. The experimental data for conductance (solid circles) were calculated numerically from the $I$–$V$ data in Fig. 2*a*. *a*, The data are fitted with the expression $dI/dV = eV/[(eV)^2-\Delta^2]^{1/2}$ (solid curve) with $\Delta = 6.8$ meV. *b*, The data are fitted with the expression $dI/dV = \mathrm{Re}[|eV-i\Gamma|/((eV-i\Gamma)^2-\Delta^2)^{1/2}]$ which includes broadening by $\Gamma$. The values of $\Delta$ and $\Gamma$ are 6.6 and 0.6 meV, respectively.

no energy gap is observed for $T \geq 30$ K. At present we do not have sufficient data to determine whether $\Delta(T)$ for $Rb_3C_{60}$ has a BCS-like temperature dependence, although it is clear that the energy gap does not persist above $T_c$. We believe that our most important finding is that the value of the low-temperature reduced energy gap for $Rb_3C_{60}$, $2\Delta/k_BT_c = 5.3$, is significantly larger than the weak-coupling prediction of 3.53. Our data thus show that the coupling, presumably to phonons, is fairly strong in the alkali-metal-doped $C_{60}$ superconductors. In previous studies of strong-coupling superconductors it has been noted that low-frequency phonon modes affect $\Delta$ more than high-frequency vibrations[17,21]. Hence, it is interesting to speculate whether, in this molecular-based superconductor, $C_{60}$–$C_{60}$ intermolecular modes give rise to the strong coupling determined from our tunnelling studies.

Most of the experimental data for alkali-metal-doped $C_{60}$ superconductors have been interpreted in terms of BCS theory with variations in $T_c$ determined by the density of electronic states at the Fermi level[2,4,9,13]. It is apparent that these analyses should at least be re-scaled by the value of $\Delta$ measured experimentally. In addition, if $T_c$ is indeed determined solely by the density of states at the Fermi level, we expect that the value of $\Delta$ found here for $Rb_3C_{60}$ will be representative of $C_{60}$ superconductors in general. It will therefore be interesting in future to investigate both the energy gap in $K_3C_{60}$ and the electron–phonon spectral function for the alkali-metal-doped $C_{60}$ superconductor. □

Received 27 August; accepted 4 September 1991.

1. Hebard, A. F. *et al. Nature* **350,** 600–601 (1991).
2. Rosseinsky, M. J. *et al. Phys. Rev. Lett.* **66,** 2830–2832 (1991).
3. Holczer, K. *et al. Science* **252,** 1154–1157 (1991).
4. Holczer, K. *et al. Phys. Rev. Lett.* **67,** 271–274 (1991).
5. Zhou, O. *et al. Nature* **351,** 462–464 (1991).
6. Benning, P. J., Martins, J. L., Weaver, J. H., Chibante, L. P. F. & Smalley, R. E. *Science* **252,** 1417–1421 (1991).
7. Stephens, P. W. *et al. Nature* **351,** 632–634 (1991).
8. Schirber, J. E. *et al. Physica* C**178,** 137–140 (1991).
9. Sparn, G. *et al. Science* **252,** 1829–1831 (1991).
10. Tanigaki, K. *et al. Nature* **352,** 222–223 (1991).
11. Kelty, S. P., Chen, C. C. & Lieber, C. M. *Nature* **352,** 223–225 (1991).
12. Chen, C. C., Kelty, S. P. & Lieber, C. M. *Science* **253,** 886–888 (1991).
13. Fleming, R. M. *et al. Nature* **352,** 787–788 (1991).
14. Kirtley, J. R. *Int. J. mod. Phys.* **4,** 201–237 (1990).
15. Bardeen, J., Cooper, L. N. & Schrieffer, J. R. *Phys. Rev.* **108,** 1175–1204 (1957).
16. Wolf, E. L. *Principles of Tunnelling Spectroscopy* (Oxford University Press, New York, 1989).
17. Hawley, M. E. *et al. Phys. Rev. Lett.* **57,** 629–632 (1986).
18. Huang, Q. *et al. Nature* **347,** 369–372 (1990).
19. Haddon, R. C. *et al. Nature* **350,** 320–321 (1991).
20. Dynes, R. C., Narayanamurti, V. & Garno, J. P. *Phys. Rev. Lett.* **41,** 1509–1512 (1978).
21. Mitrovic, B., Leavens, C. R. & Carbotte, J. P. *Phys. Rev.* B**21,** 5048–5054 (1980).

ACKNOWLEDGEMENTS. We thank D. W. Murphy (AT&T) for communication of results before publication. C.M.L. acknowledges support of this work by the David and Lucile Packard, National Science, A. P. Sloan, and Camille and Henry Dreyfus Foundations.

# Visible light emission due to quantum size effects in highly porous crystalline silicon

**A. G. Cullis & L. T. Canham**

DRA Electronics Division, Royal Signals & Radar Establishment, St Andrews Road, Malvern, Worcester WR14 3PS, UK

**LIGHT-emitting devices based on silicon would find many applications in both VLSI and display technologies, but silicon normally emits only extremely weak infrared photoluminescence because of its relatively small and indirect band gap[1]. The recent demonstration of very efficient and multicolour (red, orange, yellow and green) visible light emission from highly porous, electrochemically etched silicon[2,3] has therefore generated much interest. On the basis of strong but indirect evidence, this phenomenon was initially attributed to quantum size effects within crystalline material[2], but this interpretation has subsequently been extensively debated. Here we report results from a transmission electron microscopy study which reveals the structure of the porous layers that emit red light under photoexcitation. Our results constitute direct evidence that highly porous silicon contains quantum-size crystalline structures responsible for the visible emission. We show that arrays of linear quantum wires are present and obtain images of individual quantum wires of width <3 nm.**

The current interest in fabricating low-dimensional semiconductor structures relies upon quantum size effects which can greatly alter the properties of bulk semiconductors and have, thereby, given rise to a new generation of electronic devices. It has recently been suggested[2,4] that certain types of porous silicon can show two-dimensional carrier confinement and constitute a crystalline quantum wire array. Many workers, however, have interpreted data on porous silicon in terms of a crystallinity that deteriorates with increasing porosity and decreasing dimensionality[5]. There has even been speculation that porous silicon contains an amorphous phase in its as-anodized state[6–9]. It is, therefore, important to distinguish between these possibilities and to determine the origin of the light emission.

Porous silicon is affected by atmospheric impregnation at room temperature[10], and all characterization techniques need to take this into account. Highly porous silicon is also fragile and very chemically reactive (L.T.C., unpublished data). Previous transmission electron microscope (TEM) studies[11–15] have successfully revealed the morphology of low- to medium-porosity layers in specimens prepared by sequential mechanical